



Full Length Article

Molecular Mechanism for the Modified Sweetness and Stability of Single-Chain Sweet-Tasting Protein Monellin

Meng Zhao¹, Liu Yang¹, Bo Liu¹ and Tianming Liu^{2*}

¹School of Food Science & Engineering, Qilu University of Technology (Shandong Academy of Sciences), No. 3501 University Road of Changqing District, 250353, Jinan, Shandong Province, China

²School of Bioengineering, Qilu University of Technology (Shandong Academy of Sciences), No. 3501 University Road of Changqing District, 250353, Jinan, Shandong Province, China

*For correspondence: yanglliu@126.com; liutm2008@163.com

Abstract

The sweet-tasting protein monellin is an intensely sweet protein, which consists of two chains A and B. The single-chain monellin is folded with an α -helix and an antiparallel β -sheet, showing same sweetness with the native protein. Although many amino acid sites affecting its properties have been reported, the mechanism for the sweetness and stability of the protein is still elusive. In this study, we analyzed four mutants E23A, C41A, T12A and T12A/V37A, which exhibit variable sweetness or stability. The C41A showed slight increased sweetness and the E23A displayed substantial enhanced stability, respectively. Circular dichroism and molecular dynamics indicated that the reduced conformational flexibility at the hydrophobic core of the protein is responsible for the increased stability of E23A. Furthermore, compared with T12A and V37A, the T12A/V37A mutant led to a loss of sweetness, suggesting an important role of the intro-molecular interactive network for the sweetness of the protein. Molecular dynamics suggested that conformational changes at the N-terminal of α -helix and the C-terminal poly-(L-proline) II Helix could be the determinant for the variation of sweetness. These results provide the structural basis for the sweetness and stability of monellin protein, which could be guideline for effective modification of sweet-tasting proteins. © 2019 Friends Science Publishers

Keywords: Single-chain monellin; MNEI; Sweetness; Thermostability; Molecular dynamics

Introduction

The sweet protein monellin was isolated from the fruit of the West African shrub serendipity berry (*Dioscoreophyllum cumminsii*) in 1969 (Kohmura *et al.*, 1990). The native monellin has a molecular weight of 10.7 kDa and two non-covalently associated polypeptide chains: an A chain sequence with 44 amino acid residues, and a B chain with 50 residues. However, it has low tolerance at high temperatures or at extremes of pH (Kim *et al.*, 1989). Single-chain monellin protein (MNEI) was constructed by linking the two natural chains with a Gly-Phe dipeptide. Compared with the native protein, the MNEI has retained sweetness but shows increased thermostability. The MNEI gene has successfully been transformed and heterologously expressed in *E. coli* and yeast strains, and the recombinant construct has been extensively used in mutagenesis analysis to research the relationship between the structure and function for this protein (Temussi, 2006; Leone *et al.*, 2015).

NMR and crystallography studies have been performed to reveal the spatial structure of the native monellin protein which consists of five β -strands (β 1- β 5)

that form an antiparallel β -sheet and a 17-residue α -helix cradled in the concave face of strands (β 2- β 5). The A chain forms three of the β -strands and B chain forms two β -strands separated by the α -helix (PDB: 4MON) (Hobbs *et al.*, 2007). Of note, the solution structure of MNEI (PDB: 1IV9) is almost same to the solid structure of native protein, consistent to the results that MNEI showed the similar sweetness threshold with the native protein (Spadaccini *et al.*, 2001). Moreover, By comparison of the structures of monellin and two widely studied sweet-tasting proteins thaumatin (PDB: 1RQW) (Ohta *et al.*, 2008) and brazzein (PDB: 2LY5) (Nagata *et al.*, 2013), a common fold that 1-3 α -helix are packed with several-stranded antiparallel β -sheet was found in the configurations of these sweet-tasting proteins. Therefore, it is proposed that the relative packing arrangement of the α -helix and β -strands as well as their crystal contacts may be a determinative for the sweetness of these sweet-tasting proteins.

The molecular mechanism by which sweet-tasting proteins elicit their sweetness has been a fascinating subject for decades (Temussi, 2005). There is no sequence similarity among the sweet-tasting proteins reported until now (Wintjens *et al.*, 2011). Previous studies suggest that

the overall net charge on the protein surface can affect the sweetness, and mutants of the positive charge residues on the surface to negative charge residues result in greatly decreased sweet potency (Xue *et al.*, 2006, 2009). We have reported that the electrostatic properties of the sweet taste receptors between human and squirrel monkey probably mediate the species-dependent response to sweet-tasting proteins monellin and thaumatin (Liu *et al.*, 2012). However, mutants of the residues located in the hydrophobic core could also influence the sweetness and stability of the protein (Aghera *et al.*, 2012). Furthermore, an interesting study pointed out that the hydrophobic interaction network in the MNEI could mediate its sweetness. The researchers also suggested that increased protein flexibility and disruption of the distant poly-(L-proline) helix are involved in the sweetness of the sweet protein (Templeton *et al.*, 2011). Recently, we reported that the thermostability of MNEI can be improved with no sweetness decrease by means of gene mutagenesis and protein engineering (Liu *et al.*, 2016).

Nevertheless, full understanding of the molecular mechanism of the sweetness and stability of sweet-tasting proteins remains still limited up to now. In this study, we analyzed several key amino acids of MNEI which affect its sweetness or stability by circular dichroism and molecular dynamics, and revealed the molecular basis for the modulation of sweetness and thermostability of the sweet-tasting protein.

Materials and Methods

Constructs

The 294 bp full-length sequence of the recombinant monellin (MNEI) was from the Genbank database (Accession number: AFF58925.1). The gene was synthesized by the Genescript Biology Co. and its codon usage was optimized to facilitate the expression in *E. coli*. The gene was then digested by restriction enzymes *NdeI* and *BamHI* and cloned into the vector pET15b. The recombinant vector was checked by DNA sequencing.

Expression and Purification of the Monellin Protein

An overnight culture of *Escherichia coli* BL21-CodonPlus (DE3)-RIL harboring the recombinant vector in LB medium for 12 h at 37°C was diluted to 1:100 and then inoculated into 300 mL LB medium. The culture was induced with 0.4 mM IPTG when the OD₆₀₀ value was 0.6. The induced cells were grown for 4 h at 37°C and were centrifuged at 10000 rpm for 20 min at 4°C, then resuspended in phosphate buffer (pH 7.4) and then disrupted by sonication. The supernatant was loaded on a nickel column (Ni Sepharose™ High Performance). The recombinant proteins were eluted with the buffer containing 150 mM imidazole. The purified proteins were dialyzed with distilled water (pH 6.8) and

analyzed by 15% SDS-PAGE (Liu *et al.*, 2016). The concentration of proteins was measured by the Bradford (1976) method.

Site-directed Mutagenesis

The MNEI single-site or double-sites mutants were generated according to the overlap PCR mutagenesis method (Stratagene). The following site mutants were constructed according to the structural analysis: T12A, T12A/V37A, E23A and C41A. The MNEI variants were constructed on the basis of the recombinant vector. The following primers were synthesized to amplify the MNEI gene via PCR (Table 1). The amplified gene was mixed with the DpnI (restriction enzyme) and then transformed and cultured in *E. coli* DH5 α . The recombinant constructs were proved by sequencing analysis. All mutants were expressed and purified as the experimental procedures for wild-type protein described above.

Sweetness Threshold Assay

To evaluate the sweetness of wild-type and mutated MNEI, double-blind taste assays were carried out by a panel of 10 healthy tasters (5 males and 5 females, 20–40 old) who have normal sense of taste (Assadi-Porter *et al.*, 2000). The stored proteins were diluted by distilled H₂O (pH 6.8) at room temperature before the evaluation. A group of samples at concentrations from 0.1 to 10 μ g/mL was tested by each taster. Protein samples were evaluated from the lowest concentration. The sweetness detection threshold was defined as the lowest concentration at which the assessors perceived the sweetening power.

Thermostability

100 μ L of MNEI and its variants proteins were preheated at 40, 45, 50, 55, 60, 65, 70, 75, 80, 85 and 90°C for up to 10 h, respectively. The proteins were then taken at 2 h interval, centrifuged and analyzed by SDS-PAGE to assess the protein solubility and aggregates (Rega *et al.*, 2015). The protein thermostability was expressed as the minimum temperature at which the protein displayed complete denaturation.

Circular Dichroism

Circular dichroism (CD) spectra were measured in the potassium phosphate buffer (20 mM potassium phosphate, pH 7) on a Jasco-810 spectropolarimeter at 25°C. A 200 μ L each sample (0.1 mg/mL) was applied on CD spectra from 190–260 nm (1 mm optical path length). The spectra were recorded with an interval of 4 s and a rate of scan at 100 nm/min (0.5 nm band width). Molar ellipticity was derived according to the calculation: $[\theta](\text{deg}\cdot\text{cm}^2\cdot\text{dmol}^{-1}) = \theta_{\text{obs}} * \text{Mar}/C * l$, in which θ_{obs} is the determined ellipticity

Table 1: Primers used for construction of the MNEI mutants

Mutants	Primers
E23A sense	5' CGCGGTGGATGAAGCAAATAAAATCGGCCAG 3'
E23A antisense	5' CTGGCCGATTTTATTTGCTTCATCCACCGCG 3'
C41A sense	5'CAAAGTTATTCGCCCGCCATGAAGAAAACCATC 3'
C41A antisense	5' GATGGTTTTCTTCATGGCCGGCGAATAACTTTG 3'
T12A sense	5'CGATATTGGCCCGTTTGCCCAAGACCTGGGTTAAATTC 3'
T12A antisense	5'GAATTTACCCAGGTTCTGGGCAAACGGGCCAATATCG 3'
T12A/V37A sense	5' CTGACCTTAACAAAGCTATTGCGCCGTGCATG 3'
T12A/V37A antisense	5' CATGCACGGGCGAATAGCTTTGTAAAGGTCAG 3'

(degrees at wavelength obs), M_w is the average MW (molecular weight) of amino acids, C is the sample concentration and l is the optical path length in the assay (Sung *et al.*, 2001).

Molecular Dynamics

Four groups of simulations, the wild-type protein and three mutants (E23A, C41A and T12A/V37A) were implemented. The initial wild-type conformation was abstracted from Protein Data Bank (PDB: 1IV9). The conformations of three mutants were constructed by the Modeller program with the wild-type structure as the template (Sali and Blundell, 1993). The force field of Charmm27 was used to build proteins (MacKerell *et al.*, 2000). The protonated conditions of side chains were indicated by appointing neutral aqueous environment, where acidic residues Asp and Glu were in negative charge, while the basic residues Lys and Arg were in positive charge. There are no histidine residues in the system. Sodium and chloridion ions were added as counter ions to keep the overall neutrality. The TIP3P model was selected for water (Sun and Kollman, 1995). H₂O (in the PDB structure) was remained and additional molecules were supplied to model the aqueous environment. Periodic boundary environment were made in a rectangular periodic box, in which its initial side lengths were set to be 12 Å (the nearest distance from sample atoms to box boundaries) (de Leeuw *et al.*, 1980). The PME (Smooth Particle-Mesh Ewald) on GPU at size 64×64×64 was performed to deduce the electrostatic interactions (Harvey and De Fabritiis, 2009a; Harvey *et al.*, 2009b). The PME analyses were conducted every 2 integration steps. The switch function (9 Å and 7.5 Å cutoff) were selected to process the van der Waals interactions. The covalent bonds (composed of a hydrogen atom and a heavy atom) were confined at optimal lengths. Masses of hydrogen were multiplied (a factor of 4) a long integration (a 4 fs time step) could be applied. Subsequently, the systems were processed with energy minimization (500 steps) and 100 ps of NVT MD simulation thus the system temperature was improved to 300 K, and then another 1 ns NPT simulation for equilibration. MD simulations were performed with the program ACEMD (Harvey *et al.*, 2009b), in which the GPU hardware could be sufficiently used (GTX960). The systems were simulated along 100 ns freely to collect the configurations. Configurations were obtained every 4 ps for

the following analyses. The PYMOL program was used for molecular graphics (Seeliger and de Groot, 2010).

Results

Analysis of the Intra-molecular Interaction of Single-chain Monellin Protein

Previous studies showed that mutants of G16A and V37A led to 10 and 2 times reduction of the sweetness of MNEI, respectively, while G16A/V37A resulted in 4 times reduction of sweetness. These results suggest the correlation between G16 and V37 which are involved in the intermediate interactive network in the protein (Templeton *et al.*, 2011). The authors also proposed that the effect of hydrophobic interaction network could be propagated to affect the conformational flexibility of C-terminal poly-(L-proline) II Helix, which was responsible for the variation in sweetness. In the protein's structure, G16 and V37 interact via the hydrophobic forces, and residue T12 is hydrogen bonded with G16. Therefore, T12 could interact with V37 through the intermediate interactive network *via* G16 (Fig. 1). To test this hypothesis, we constructed a single-site mutant (T12A) and a double-sites mutant (T12A/V37A). Furthermore, we have recently reported two variants E23A and C41A displaying increased sweetness and thermostability, respectively (Liu *et al.*, 2016). The molecular mechanism of the altered properties of these variants was investigated as below.

Expression and Purification of the Wide-type and Variants of MNEI

One double-site and three single-site mutants of MNEI were constructed and expressed in *Escherichia coli* BL21-CodonPlus (DE3)-RIL. The double-sites mutant T12A/V37A and single-site mutants T12A, E23A and C41A were successfully expressed and purified as shown in Fig. 2.

Sweetness Sensory

The sweet potency of mutants T12A, T12A/V37A, E23A, C41A and wild-type MNEI were evaluated as depicted in "Materials and methods".

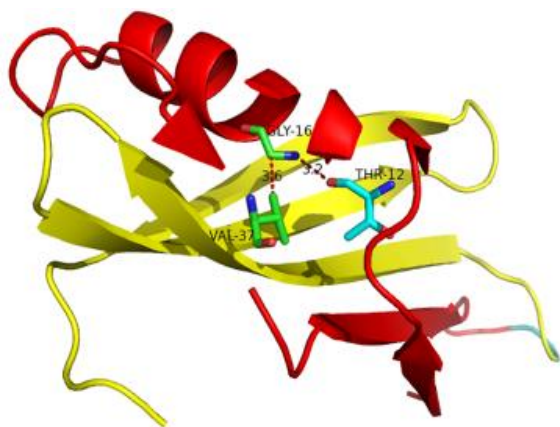


Fig. 1: Intra-molecular interaction between T12 and V37 via G16 in the single-chain monellin. The A and B chains are colored in yellow and red, respectively. Residues are shown in stick mode and colored by atom types. The interactions between the residues are denoted as red dash lines with the indicated distance (Å)

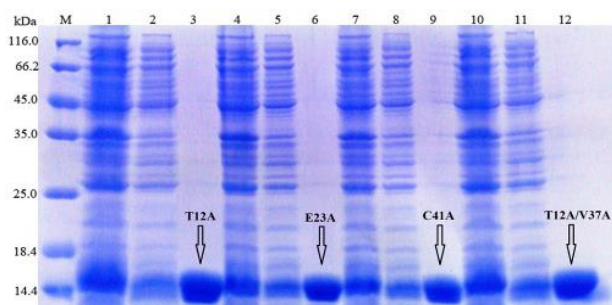


Fig. 2: Expression and purification of the wide-type MNEI and its variants. M. molecular weight marker; 1. total protein extract of T12A; 2. the supernatant protein of T12A; 3. the single band of T12A; 4. total protein extract of E23A; 5. the supernatant protein of E23A; 6. the single band of E23A; 7. total protein extract of C41A; 8. the supernatant protein of C41A; 9. the single band of C41A; 10. total protein extract of T12A/V37A; 11. the supernatant protein of T12A/V37A; 12. the single band of T12A/V37A

The results showed that compared to the wild-type monellin protein (detection threshold: $1.1 \mu\text{g/mL}$), mutant of E23A had no influence on the sweetness, while mutant of C41A resulted in a slight increased sweet potency (sweetness threshold: $0.8 \mu\text{g/mL}$). The T12A mutant displayed reduced sweetness with a sweet threshold of $10 \mu\text{g/mL}$. However, the double-sites mutant T12A/V37A showed no detectable sweetness even the concentrations reached to $1000 \mu\text{g/mL}$, indicating a complete loss of its sweetness (Table 2). Comparison of the sweetness of T12A, V37A and T12A/V37A, it is revealed that combination of the two mutants (T12A and V37A) which are located at relatively far distance have negative effect on the sweetness of the protein (Templeton *et al.*, 2011).

Thermostability

The thermostability of T12A/V37A, E23A, C41A and wild-type MNEI were analyzed by heat-treatment and SDS-PAGE. The wild-type protein turned to be denatured at 65°C . The C41A mutant, which showed increased sweetness, led to a slight improvement of thermostability (about 5°C). Remarkably, the E23A mutant displayed significant improved thermostability with the minimum denaturation temperature being 85°C . The T12A/V37A mutant which tastes no sweetness, showed a decreased but retained thermostability (Table 2). These results demonstrated that the properties of the sweet-tasting protein could be modified by gene mutagenesis and protein engineering, and are in accordance with the previous findings that there is no direct correlation between the stability and sweetness of sweet-tasting proteins.

CD Spectra Analysis

Circular dichroic spectra of both wild-type and its mutants showed a major α -helix and β -stands fold of the proteins, suggesting that the global configuration and secondary structure of the variants are highly similar to that of wild-type (Fig. 3). However, compared to the wild-type, difference of small negative peaks at 208 nm and 216–218 nm were present in E23A and T12A/V37A but absent in C41A, indicating subtle conformational changes of the α -helix and β -strands region in the two mutants (E23A and T12A/V37A).

Molecular Dynamics

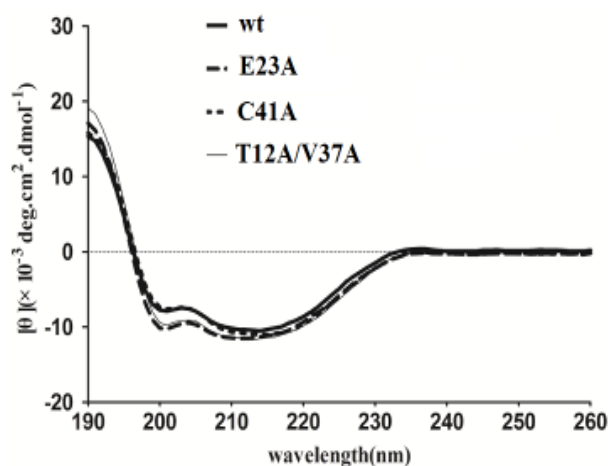
To investigate the structural basis of modified sweetness and stability of MNEI, we performed 100 ns MD simulations on the experimental structures of MNEI and the three mutants E23A, C41A and T12A/V37A. Compared with their crystal structures, the backbone atom positional Root Mean Square Deviation (RMSD) of four trajectories were stable (2~3 angstrom, Fig. 4a). The Root Mean Square Fluctuation (RMSF) per residue of the protein backbones of the four structures displayed similar patterns, indicating that the overall configurations of the proteins were retained upon the mutants added (Fig. 4b). However, high flexibility was found in correspondence of some specific residues region, which was in accordance with their variance of sweetness or stability. For instance, the C41A mutant, exhibited the most similar properties with that of the wild-type (Table 2), showing a moderate fluctuation relative to the wild-type in the RMSF analysis. The E23A mutant, with the considerably increased thermostability, displayed a significant decreased conformational flexibility in the region around residues 20–30, suggesting a more stable structure around the mutated residue. Overlap of the averaged structure of wild-type with that of E23A showed the conformational discrepancy between the two proteins (Fig. 5a).

Table 2: Sweetness threshold and stability of monellin and its mutants

Proteins	Sweetness threshold ($\mu\text{g/mL}$)	Minimum heat denaturation temperature ($^{\circ}\text{C}$)
MNEI	1.1	65
E23A	1.1	85
C41A	0.8	70
T12A	10	55
T12A/V37A	>1000	55
V16A	2 ^a	nr
V37A	10 ^a	55
V16A/V37A	4 ^a	nr

^a: see reference Templeton *et al.* 2011

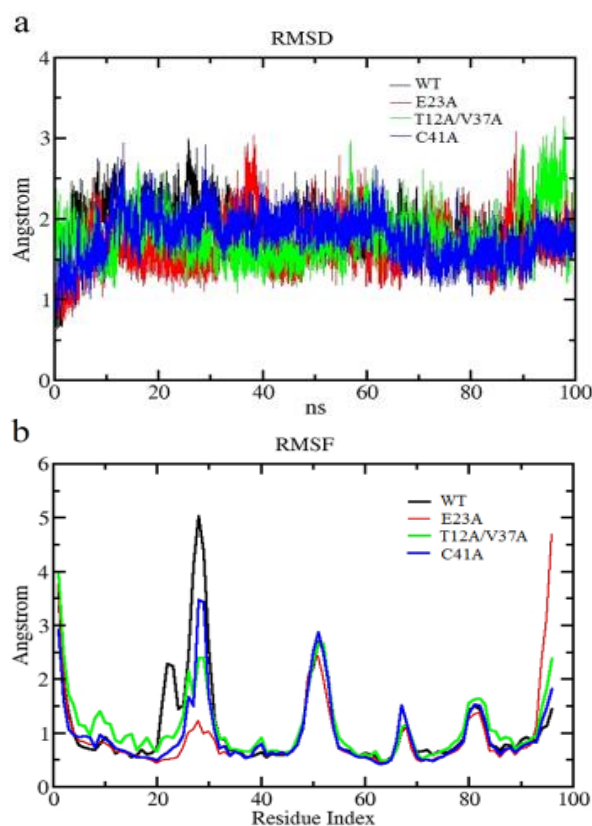
nr: not reported

**Fig. 3:** Circular dichroism spectrum of wild-type MNEI and variants E23A, C41A and T12A/V37A

The T12A/V37A double-sites mutant, which is no sweetness in taste, had a substantial effect on the motions of N-terminal of α -helix and the C-terminal poly-(L-proline) II Helix (P94-P96) (Fig. 5b). The reduced sweetness of the protein resulting from increased protein flexibility and disruption of a distant poly-(L-proline) II Helix. Based on these results, we conclude that the mutations of E23A and T12A/V37A have significant effects on its solution structure and backbone dynamics, which is the structural origin of its sweetness and stability.

Discussion

Previous findings on mutants G16A, V37A and G16A/V37A suggested that the intra-molecular interaction network is crucial for the sweetness of the sweet-tasting protein monellin. To extend this point, we analyzed a residue T12, although located relatively far from the residue V37, showing correlation but negative effect with V37 on the sweetness. Analysis of the structure revealed that T12 could interact with V37 via the G16, which can hydrogen bonded with T12 and interact with

**Fig. 4:** Molecular dynamics analysis of the wild-type MNEI and its variants. **(a)** Root Mean Square Deviation (RMSD) per residue of wild-type MNEI and variants E23A, C41A and T12A/V37A in 100 ns simulations. Different colors represent different trajectory as shown in the figure. **(b)** Root Mean Square Fluctuation (RMSF) per residue of wild-type MNEI and variants E23A, C41A and T12A/V37A

V37 through the hydrophobic forces. The results are in accordance with the previous report that the hydrophobic interaction network in monellin could be propagated and affected the protein sweetness (Templeton *et al.*, 2011). Another study has reported that the inter-chain and intra-chain interactions in the A and B chains of monellin prevent aggregation by stabilizing the native state of the protein, highlighting the relationship between the intra-molecular interaction and the stability of this protein (Szczeplankiewicz *et al.*, 2011).

Considering the folding similarity among sweet-tasting proteins (Spadaccini *et al.*, 2001; Ohta *et al.*, 2008; Nagata *et al.*, 2013), our results suggest that the intra-molecular interaction could be a determinant for the sweetness, which could probably be applied to all of the sweet-tasting proteins. This scenario could also be a guideline for effective design of novel sweet-tasting proteins and should be informative in the further investigations.

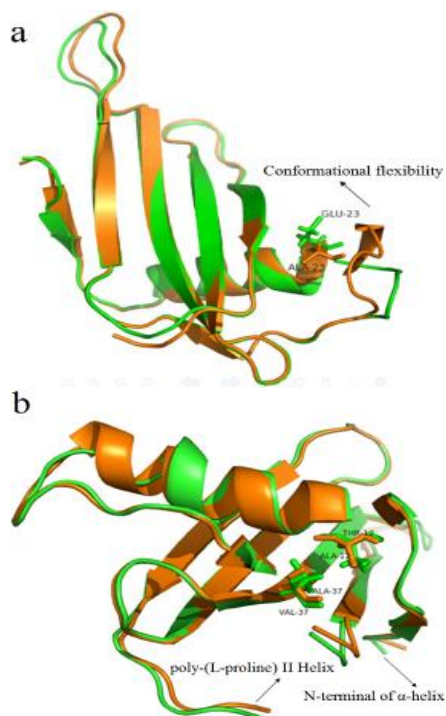


Fig. 5: Overlap the modeled average structures of wild-type MNEI and two variants. **(a)** Overlap the structures of wild-type and E23A. Wild-type MNEI and E23A were shown in green and orange, respectively. The mutated residues from E23 to A23 were rendered as stick models. The region around the mutated residue with significant conformational flexibility was denoted. **(b)** Overlap the structures of wild-type and T12A/V37A. Wild-type MNEI and T12A/V37A were shown in green and orange, respectively. The mutated residues from T12/V37 to A12/ A37 were rendered as stick models. The N-terminal of α -helix and the C-terminal poly-(L-proline) II Helix (P94-P96) with conformational flexibility were denoted

We found two mutants E23A and C41A exhibiting increased stability and sweetness, respectively. E23 residue is buried in the core of the protein and highly ionizable, and the enhancement of the thermostability of E23A is in accordance with the rationalization that replacement of this unpartnered ionizable residue from the hydrophobic core of the protein can stabilize the native state of the protein (Aghera *et al.*, 2012). The reduced flexibility of residues around the E23 in the MD analysis reflects the increased stability of E23A mutant (Fig. 4). The C41 residue is also buried in the protein core, and the MD analysis mirrored the similar properties between C41A (with slight increased sweetness) and the wild-type MNEI. A sweeter mutant Y65R located at the surface of protein has also been shown to exhibit a minimal impact on the motion of the protein (Rega *et al.*, 2015). The T12A/V37A mutant induces the conformational fluctuation and increased flexibility of the C-terminal poly-(L-proline) II Helix (P94-P96) which could interact with the sweet taste receptors thus abolish the sweetness of the wild-type protein (Templeton *et al.*, 2011).

Conclusion

Taken together, our results revealed the structural basis for the modified sweetness and stability of the single-chain monellin protein and provided guidance for effective modulation of sweet-tasting proteins.

Acknowledgments

We acknowledge the experimental support for this study from Dr. Yue Hu in the Department of Bioengineering, Qilu University of Technology.

References

- Aghera, N., I. Dasgupta and J.B. Udgaonkar, 2012. A buried ionizable residue destabilizes the native state and the transition state in the folding of monellin. *Biochemistry*, 51: 9058–9066
- Assadi-Porter, F.M., D.J. Aceti and J.L. Markley, 2000. Sweetness determinant sites of brazzein, a small, heat-stable, sweet-tasting protein. *Arch. Biochem. Biophys.*, 376: 259–265
- Bradford, M.M., 1976. A rapid and sensitive method for the quantitation of microgram quantities of protein utilizing the principle of protein-dye binding. *Anal. Biochem.*, 72: 248–254
- de Leeuw, S.W., J.W. Perram and E.R. Smith, 1980. Simulation of electrostatic systems in periodic boundary conditions. I. Lattice sums and dielectric constants. *Proc. Roy. Soc. Lond. A*, 373: 27–56
- Harvey, M.J. and G. De Fabritiis, 2009a. An implementation of the smooth particle mesh ewald method on GPU Hardware. *J. Chem. Theor. Comput.*, 5: 2371–2377
- Harvey, M.J., G. Giupponi and G.D. Fabritiis, 2009b. ACEMD: accelerating biomolecular dynamics in the microsecond time scale. *J. Chem. Theor. Comput.*, 5: 1632–1639
- Hobbs, J.R., S.D. Munger and G.L. Conn, 2007. Monellin (MNEI) at 1.15 Å resolution. *Acta Crystallogr. Sect. F: Struct. Biol. Crystall. Commun.*, 63: 162–167
- Kim, S.H., C.H. Kang, R. Kim, J.M. Cho, Y.B. Lee and T.K. Lee, 1989. Redesigning a sweet protein: increased stability and renaturability. *Protein Eng.*, 2: 571–575
- Kohmura, M., N. Nio and Y. Ariyoshi, 1990. Complete amino acid sequence of the sweet protein monellin. *Agric. Biol. Chem.*, 54: 2219–2224
- Leone, S., F. Sannino, M.L. Tutino, E. Parrilli and D. Picone, 2015. Acetate: friend or foe? Efficient production of a sweet protein in *Escherichia coli* BL21 using acetate as a carbon source. *Microb. Cell Fact.*, 14: 106
- Liu, B., M. Ha, X.Y. Meng, M. Khaleduzzaman, Z. Zhang, X. Li and M. Cui, 2012. Functional characterization of the heterodimeric sweet taste receptor T1R2 and T1R3 from a New World monkey species (squirrel monkey) and its response to sweet-tasting proteins. *Biochem. Biophys. Res. Commun.*, 427: 431–437
- Liu, Q., L. Li, L. Yang, T. Liu, C. Cai and B. Liu, 2016. Modification of the sweetness and stability of sweet-tasting protein monellin by gene mutation and protein engineering. *Biomed. Res. Int.*, 2016: 1–7
- MacKerell, A.D., N. Banavali and N. Foloppe, 2000. Development and current status of the CHARMM force field for nucleic acids. *Biopolymers*, 56: 257–265
- Nagata, K., N. Hongo, Y. Kameda, A. Yamamura, H. Sasaki, W.C. Lee, K. Ishikawa, E.I. Suzuki and M. Tanokura, 2013. The structure of brazzein, a sweet-tasting protein from the wild African plant *Pentadiplandra brazzeana*. *Acta Crystallogr. Sect. D: Biol. Crystallogr.*, 69: 642–647
- Ohta, K., T. Masuda, N. Ide and N. Kitabatake, 2008. Critical molecular regions for elicitation of the sweetness of the sweet-tasting protein, thaumatin I. *FEBS J.*, 275: 3644–3652

- Rega, M.F., R. Di Monaco, S. Leone, F. Donnarumma, R. Spadaccini, S. Cavella and D. Picone, 2015. Design of sweet protein based sweeteners: Hints from structure–function relationships. *Food Chem.*, 173: 1179–1186
- Sali, A. and T.L. Blundell, 1993. Comparative protein modelling by satisfaction of spatial restraints. *J. Mol. Biol.*, 234: 779–815
- Seeliger, D. and B.L. de Groot, 2010. Ligand docking and binding site analysis with PyMOL and Autodock/Vina. *J. Comput. Aided Mol. Des.*, 24: 417–422
- Spadaccini, R.O. Crescenzi, T. Tancredi, C.N. De Casamassimi, G. Saviano, R. Scognamiglio, D.A. Di Donato and P.A. Temussi, 2001. Solution structure of a sweet protein: NMR study of MNEI, a single chain monellin. *J. Mol. Biol.*, 305: 505–514
- Sun, Y. and P.A. Kollman, 1995. Hydrophobic solvation of methane and nonbond parameters of the TIP3P water model. *J. Comput. Chem.*, 16: 1164–1169
- Sung, Y.H., J. Shin, H.J. Chang, J.M. Cho and W. Lee, 2001. Solution structure, backbone dynamics, and stability of a double mutant single-chain monellin. structural origin of sweetness. *J. Biol. Chem.*, 276: 19624–19630
- Szczepankiewicz, O., C. Cabaleiro-Lago, G.G. Tartaglia, M. Vendruscolo, T. Hunter, G.J. Hunter, H. Nilsson, E. Thulin and S. Linse, 2011. Interactions in the native state of monellin, which play a protective role against aggregation. *Mol. Biosyst.*, 7: 521–532
- Templeton, C.M., S. Ostovar pour, J.R. Hobbs, E.W. Blanch, S.D. Munger and G.L. Conn, 2011. Reduced sweetness of a monellin (MNEI) mutant results from increased protein flexibility and disruption of a distant poly-(L-proline) II Helix. *Chem. Senses*, 36: 425–434
- Temussi, P.A., 2005. From oligopeptides to sweet proteins. *J. Pept. Sci.*, 11: 262–264
- Temussi, P.A., 2006. Natural sweet macromolecules: how sweet proteins work. *Cell Mol. Life Sci.*, 63: 1876–1888
- Wintjens, R., T.M. Viet, E. Mbosso and J. Huet, 2011. Hypothesis/review: the structural basis of sweetness perception of sweet-tasting plant proteins can be deduced from sequence analysis. *Plant Sci.*, 181: 347–354
- Xue, W.F., O. Szczepankiewicz, E. Thulin, S. Linse and J. Carey, 2009. Role of protein surface charge in monellin sweetness. *Biochim. Biophys. Acta*, 1794: 410–420
- Xue, W.F., O. Szczepankiewicz, M.C. Bauer, E. Thulin and S. Linse, 2006. Intra-versus intermolecular interactions in monellin: contribution of surface charges to protein assembly. *J. Mol. Biol.*, 358: 1244–1255

(Received 03 July 2018; Accepted 23 July 2018)